Conditioning Monitoring of a Flexible Coupling Using Experimental Data Based Modelling

Pramod N. BELKHODE
Department of General Engineering, Laxminarayan Institute of Technology, Nagpur, Maharashtra, India, pramodb@rediffmail.com

Girish D. MEHTA
Department of Mechanical Engineering, Priyadarshini College of Engineering, Nagpur, Maharashtra, India, girishm97@rediffmail.com

Sagar D. SHELARE
Department of Mechanical Engineering, Priyadarshini College of Engineering, Nagpur, Maharashtra, India, sagmech24@gmail.com

Akshay A. PACHPOR
Department of Mechanical Engineering, Priyadarshini College of Engineering, Nagpur, Maharashtra, India, pachpor.a@gmail.com

Ruma ROY
Department of Mechanical & Automation Engineering, Amity University, Kolkata, rumaroy16@gmail.com

Abstract: - The modern industrial system is built on rotating machinery. Faulty machinery significantly increases vibration, particularly in the coupling, which leads to catastrophic failure of essential machinery components and, in some cases, worker life. As a result, the fault-free operation of rotary machinery with proper alignment is the primary goal of many companies. This study attempts to establish a relationship between the amount of misalignment and the rise of vibration amplitude at pertinent coupling frequencies. For this purpose, an experimental setup was designed and developed. Also, the experimentation was carried out to predict the vibration amplitude by considering various independent variables like speed, mean bearing radius, misalignment tolerance, mass moment of inertia, moment of area, modulus of elasticity, and weights of various coupling, rotors, load drum, and shafts. The effects of these various independent variables have been portrayed in terms of a group of pi terms with the help of the dimensional analysis technique. The model for vibration amplitude was formulated by using these pie terms. A further developed model was analyzed qualitatively and quantitatively. The reliabilities of mathematical models obtained are practically superior. However, some pie terms in the mathematical models are highly sensitive whilst others are less sensitive.

Keywords: - Experimental data-based model, flexible coupling, misalignment, vibration-based prognosis.

1. INTRODUCTION

Typically rotating types of machinery are made up of three primary components: the bearings, the rotors, and the foundations [1]-[2]. Misalignment is an unavoidable condition that persists in all types of machinery. It gives rise to vibrations [3]-[4]. The vibration has a very severe effect on the operating life of a machine component and in turn, reduces productivity due to unpredictable stoppage of the machineries [5]-[6]. At least 60% of the problems in systems are due to misalignment [7]. Under the misaligned condition, when a motor shaft axis and a driven shaft axis are inclined at an angle it is known as angular misalignment. Parallel misalignment occurs when there is a parallel offset between the two axes of shafts. It can also occur as an angular and parallel misalignment [8]-[9]. The effect of misalignment has been greatly reduced by introducing the flexible coupling between a motor shaft and a driven system [10]. There are various types of flexible coupling used [11]. However, if one considers the case of two jaws elastomeric coupling, then it consists of two hubs and an elastomeric element [12]. This elastomeric or flexible element is placed between the hubs to cope with misalignment in the system [13]. So, the flexible element operates under different loads i.e driving torque from motor

and load due to misalignment [14]-[15]. It serves an important function in reducing vibration and protecting other machine components from failure [16].

The study of vibration signals, which typically conveys data of health status of rotational machinery, is used to perform condition monitoring on rotating machinery. Unfortunately, detailed assessments of obtained time-domain signals are impractical. The frequency-domain analysis gives a further straight approach for monitoring a health state, and signal processing technology are typically used to uncover faulty unseen modulations of a spectrum, hence aiding diagnosis [17]. Edwards et al. [18] provided a concise overview of the larger area of fault diagnostics. Muszynska [19] provided an in-depth examination of investigation of the rotor-stator rub phenomenon. Foiles et al. [20] and Parkinson [21] provided in-depth evaluations of rotor rebalancing. Schweitzer and Maslen Schweitzer suggested alternative control algorithms for rigid and flexible rotor systems and fault variables estimation [22]. Lees [23] discussed the periodic disturbances of coupled rotor with idealized continuous bearings, rigid rotors, and stiff coupling. The research of rotor misalignment has indeed been restricted to a qualitative knowledge of a phenomena [24]-[26], however no method for direct measurement of misalignment defects has been proposed.

Kuppa and Lal [27-28] and Lal and Tiwari [29] describe coupling with respect to angular and linear stiffness, as well as linear damping. They ignored a speed dependence of the bearing and coupling in their calculations. Lal and Tiwari [30] included the speed dependence of bearing and coupling into the simulation. They have not, however, approximated the speed-dependent characteristics. The rotating machine was subjected to vibration analysis and condition monitoring by Vishwakarma et al. [31]. They introduced extracting features approaches for detecting vibration in several types of rotating machinery in this research. Sawalhi et al. [32] used finite element simulation to model and diagnose misalignment of a vibration test apparatus. They came to the conclusion that shaft harmonic deviation may enhance vibration acceleration of high order. Kuppa and Lal [33-34] devised a continuous condition monitoring approach for addressing a misalignment issue of rotational equipment; authors also evaluated a coupling and bearing characteristics, as well as the controller's characteristics. Lal and Satapathy [35] investigate a speed dependency of coupling and bearing combined for the first time.

Based on the literature review results, it is possible to infer that fault of coupling misalignment are mostly calculated in terms of the damping and stiffness characteristics of the element, which has been a accepted technique for estimation since several decades. Harmonic excitation in rotating equipment is caused by rotational imbalance, coupling misalignment, bearing flaws, and shaft fractures [36]-[40]. Even though it is aware that misalignment of coupling varies with vibration, the vibration amplitude-dependent phenomenon of flexible coupling has hitherto been overlooked. Thus, it became essential to study the vibration behavior of the flexible element of the coupling under misalignment conditions.

In the present article, the vibration behavior of the flexible element of the coupling under misalignment conditions has been studied. For this, effects of various independent variables have been portrayed in terms of a group of pi terms with the help of dimensional analysis technique, and a model for vibration amplitude was formulated. Also, sensitivity analysis has been performed to find out highly sensitive variables.

2. MISALIGNMENT VIBRATIONS

When the shafts are coupled, they fall under cyclic strain and this is the real cause of vibration. It is also studied that as the misalignment in the coupling increases, the vibration amplitude does not increase linearly [41]-[42]. This happens because during rotation, when one flange of coupling wants to deflect in one direction, it pulls the other flange with it. This deflection creates the vibration amplitude at coupling frequencies, but the other flange pulls it back to come at the centerline. This prevents the growth of amplitude at pertinent frequencies. This action lasts for every cycle of the shaft rotation [43]. If one refers to Figures (1, 2, 3), then the deflection of a flange occurs due to the misalignment condition [44]. This deflection creates additional moments at joints, which then converts into the reaction at the bearings.

These increased reactions are mainly responsible for inducing the amplitude [45]. But when the other flange pulls the first flange, the reactions in the bearings get reduced.

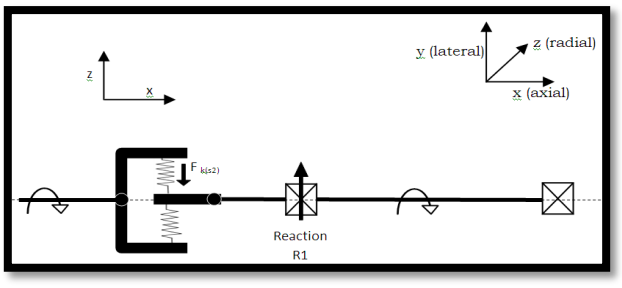

Figure 1. The reaction produced in an aligned system

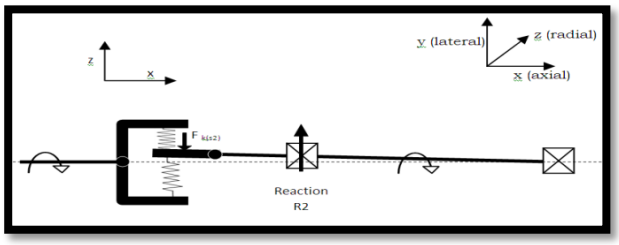

Figure 2. The reaction produced due to stiffness of the elastomeric element

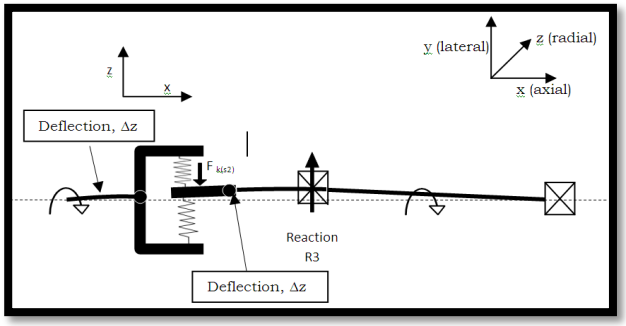

Figure 3. The reaction produced due to combining effect of deflection in the shaft and elastomeric element stiffness

3. MISALIGNMENT AND VIBRATION AMPLITUDE

The general assumption is that the increase in misalignment should increase amplitudes at pertinent frequencies of coupling, but in practice it shows non-linearity i.e initially if one notes down the values of amplitudes at pertinent frequencies of coupling for a known value of misalignment, further he then increased the amount of misalignment double of the initial amount and note down the values of amplitudes at the same frequencies then that would not be the double of initial amplitude values [46].

There is no such relationship that exists between the amount of misalignment and vibration amplitude [43]. In the prowl of a technique to form this relationship, the present work is propelled towards the formulation of a mathematical model.

In this regard an experiment has been carried out which is as under:

3.1. Experimental setup

Figure. 4 shows a schematic arrangement of the experimental setup designed and developed for experimentation purposes.

In this configuration, an electric motor with a rated capacity of 0.5 hp is employed. The purpose of mounting these rotors on the shaft is to create load on the bearings. Shaft S2 houses the two rotors R1, R2, and the load drum BRD.

A motor shaft S1 is connected to a shaft S2 by a two-jaw elastomeric coupling JC [47]. The shaft S2 is supported by two ball bearings B1 and B2. A provision of load drum BRD is placed at the end of shaft S2. The shaft S2 assembly is fastened to the two bearing B1 and B2 pedestals using nuts and bolts [48]. These two pedestals are already mounted on a cast iron plate measuring 800 mm x 200 mm x 20 mm. However, the structure is also constructed in the experimental setting to provide misalignment in the radial and lateral directions.

Figure 5 shows a actual experimental setup with an accelerometer attached at bearing for acquiring the readings [49]. The setup specifications are given in table 1.

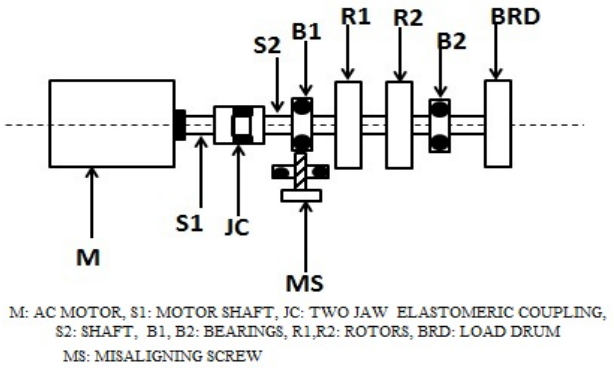

Figure 4. Schematic diagram of an experimental setup

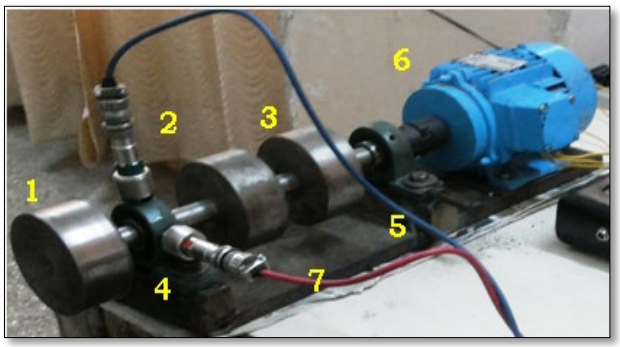

Figure 5. Pictorial view of experimental setup

Where,1-Load drum (BRD), 2-Rotor (R1), 3-Rotor (R3), 4-Bearing (B2), 5-Bearing (B1), 6-Motor (M), 7-Shaft (S2)

Table 3. Dimensions of machine components

Sr. No.	Description	Unit
1	Shaft (S2) diameter	25 mm
2	Shaft (S2) Length	300 mm
3	Rotor weight (R1, R2)	2 kg
4	Load drum weight (BRD)	2 kg
5	Width of the jaw	10 mm
6	Inner diameter of jaw	10 mm
7	Outer diameter of jaw	25 m

3.2. Model formulation

The quest for further development in the present work, basically confronted with a better analytical technique. This analytical technique is a formulation of a mathematical model which can predict the vibration amplitudes at coupling frequencies [50]-[51]. Indeed, any physical occurrence can be represented by a mathematical assessment obtainedby learning the connection between effects and causes, which will be known as a mathematical prototype. The forthcoming articles will elaborate on the procedure for the formulation of a mathematical model.

3.3. Process of model formulation

Some important steps involved in the process of prototype invention are as follows [52]-[53] (Schenck, 1967)

3.3.1 Variables identification

The first step is the recognition of variables in the model invention process. The dependent/ independent variables identified are given in table 2.

Table 4. List of Independent and Dependent Variables

Variable Type	Variable	Form of MLT	Symbol
Dependent	Vibration amplitude	LT^{-1}	Y
Independent	Speed	T^{-1}	N
Independent	Mean bearing radius	L	R_{mb}
Independent	Mass moment of Inertia of coupling, rotor1, rotor 2, and load drum	ML^2	I_c, I_{r1}, I_{r2}, I_{r3},
Independent	Second moment of area of shaft S1 and S2.	L^4	I_{s1} , I_{s2}
Independent	Modulus of elasticity coupling, rotor1, rotor2, load drum, shaft S1, shaft S2.	$ML^{-1}T^{-2}$	E_c, E_{r1}, E_{r2}, E_{r3}, E_{s1}, E_{s2}
Independent	Equivalent distances	L	L_{e1},L_{e2}, L_{e3}, L_{e4}, L_{e5}, L_{e6}
Independent	Load Torque	ML^2T^{-2}	T_L
Independent	Acceleration due to gravity	LT^{-2}	G
Independent	Time	T	T
Independent	Misalignment tolerance	L	H_m, V_m
Independent	Weight of coupling, rotor 1, rotor2, load drum, shaft S1, shaft S2	MLT^{-2}	W_c, W_{r1}, W_{r2}, W_{r3}, W_{s1}, W_{s2}

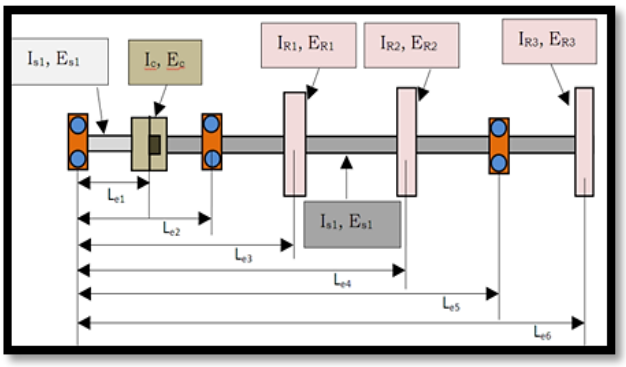

Figure 6. Schematic diagram of equivalent system

The variables itemized in table 2 can be classified as Autonomous variables (causes), Reliant variables (effects), and extraneous variables. Here, the designer has a choice to introduce some variations in the autonomous variables while the variation in the reliant variable totally depends on variation in the autonomous variable. The extraneous variables are the variables on which cannot be controlled. For more interpretation, the variables corresponding to individual machine components are depicted in Figure 6.

3.3.2. Reduction of variables through dimensional analysis

In this step all the identified autonomous variables are reduced to a group of Pi (π) terms. This can be achieved by following dimensional assessment technique [54]-[55]. The basic steps in this technique are

a. Recognition of variables,

b. Use of Religh's method, to get the reliant and autonomous pi terms.

$$Y = f\,(I_C, I_{R1}, I_{R2}, I_{R3}, I_{S1}, I_{S2}, E_C, E_{R1}, E_{R2}, E_{R3}, E_{S1}, E_{S2}, L_{e1}, L_{e2}, L_{e3}, L_{e4}, L_{e5}, L_{e6}, W_c, W_{R1}, W_{R2}, W_{R3}, W_{S1}, W_{S2}, N, t, H_m, V_m, R_{bm}, T_L, g), \quad (1)$$

$$Y= f\,[(I_C)^{a1},\ (I_{R1})^{a2},\ (I_{R2})^{a3},\ (I_{R3})^{a4},\ (I_{S1})^{a5},\ (I_{S2})^{a6},\ (E_C)^{b1},\ (E_{R1})^{b2},\ (E_{R2})^{b3},\ (E_{R3})^{b4},\ (E_{S1})^{b5},\ (E_{S2})^{b6},\ (L_{e1})^{c1},\ (L_{e2})^{c2},\ (L_{e3})^{c3},\ (L_{e4})^{c4},\ (L_{e5})^{c5},\ (L_{e6})^{c6},(W_c)^{d1},(W_{R1})^{d2},\ (W_{R2})^{d3},\ (W_{R3})^{d4},\ (W_{S1})^{d5},\ (W_{S2})^{d6},(N)^e,\ (t)^f,\ (H_m)^g,\ (V_m)^h,\ (R_{bm})^i,\ (T_L)^j,\ (g)^k] \quad (2)$$

$$[LT^{-1}] = [ML^2]^{a1+a2+a3+a4+a5+a6}\,[ML^{-1}T^{-2}]^{b1+b2+b3+b4+b5+b6}\,[L]^{c1+c2+c3+c4+c5+c6}\,[MLT^{-2}]^{d1+d2+d3+d4+d5+d6}\,[T^{-1}]^e\,[T]^f[L]^g\,[L]^h\,[L]^i\,[ML^2T^{-2}]^j\,[LT^{-2}]^k \quad (3)$$

For M:

$$0=a1+a2+a3+a4+a5+a6+b1+b2+b3+b4+b5+b6+d1+d2+d3+d4+d5+d6+j \quad (4)$$

For L:

$$1=2(a1+a2+a3+a4+a5+a6)-(b1+b2+b3+b4+b5+b6)+(c1+c2+c3+c4+c5+c6)+(d1+d2+d3+d4+d5+d6)\ +g+h+i+2j+k \quad (5)$$

For T

$$-1 = -2(b1+b2+b3+b4+b5+b6)-2(d1+d2+d3+d4+d5+d6)-e+f-2j-2k \quad (6)$$

Now by simplifying one will get,

$$\frac{Y}{NRmb} = \left[\frac{I_{r1}}{I_c}\frac{I_{r2}}{I_{r3}}\frac{I_{s2}}{I_{s1}}\frac{W_{r1}}{W_c}\frac{W_{r2}}{W_{r3}}\frac{W_{s2}}{I_{s1}}\right]^a\left[\frac{E_{r1}}{E_c}\frac{E_{r2}}{E_{r3}}\frac{E_{s2}}{E_{s1}}\right]^b\left[\frac{I_{e2}}{I_{e1}}\frac{I_{e4}}{I_{e3}}\frac{I_{e6}}{I_{e5}}\right]^c\frac{H_m}{V_m}\frac{t}{g}\frac{NR_{mb}T_L}{I_c}\Big]^d \quad (7)$$

The above equation can be represented in the form of pie (π) terms as:

$$\pi = \pi_1^a\pi_2^b\pi_3^c\pi_4^d \quad (8)$$

where,

$\pi_1 = \left[\frac{I_{r1}}{I_c}\frac{I_{r2}}{I_{r3}}\frac{I_{s2}}{I_{s1}}\frac{W_{r1}}{W_c}\frac{W_{r2}}{W_{r3}}\frac{W_{s2}}{I_{s1}}\right]$,

$\pi_2 = \left[\frac{E_{r1}}{E_c}\frac{E_{r2}}{E_{r3}}\frac{E_{s2}}{E_{s1}}\right]$,

$\pi_3 = \left[\frac{L_{e2}}{L_{e1}}\frac{L_{e4}}{L_{e3}}\frac{L_{e6}}{L_{e5}}\right]$,

$\pi_4 = \left[\frac{H_m}{V_m}\frac{t}{g}\frac{NR_{mb}T_L}{I_c}\right]$

Equation (8) π represents dependent variable which denotes vibration amplitude and π_1, π_2, π_3, π_4 are independent pie terms which represent mass moment of inertia, elasticity, equivalent length and dynamic characteristics of the equivalent system respectively.

3.3.3. Test Planning

Test envelope

The test envelopes for values of Pie terms of six different mathematical models are tabulated in Table 3 to Table 8.

Table 5. The Values of Different Range of Test Points for π1, π2, π3, π4

Terms	π1	π2	π3	π4
For dependent pi term of Model 1Xh†				
Minimum	704.040	1.05	1.900000	62.3
Maximum	704.040	1.05	1.900000	159777.3
For dependent pi term of Model 2Xh‡				
Minimum	704.040	1.05	1.900000	62.3
Maximum	704.040	1.05	1.900000	159777.3
For dependent pi term of Model 3XhΔ				
Minimum	704.040	1.05	1.900000	62.3
Maximum	704.040	1.05	1.900000	159777.3
For dependent pi term of Model 1Xv$				
Minimum	704.040	1.05	1.900000	62.3
Maximum	704.040	1.05	1.900000	159777.3
For dependent pi term of Model 2Xv□				
Minimum	704.040	1.05	1.900000	62.3
Maximum	704.040	1.05	1.900000	159777.3
For dependent pi term of Model 3Xv†				
Minimum	704.040	1.05	1.900000	62.3
Maximum	704.040	1.05	1.900000	159777.3

Test points

During experimentation, the experimental setup is set for the discreet of independent pie terms. These values are referred to as test points, and they are normally confined inside the domain of the test envelope [56]. The table 9 shows test points of the present work.

Table 4. Different Test Points for π1, π2, π3and π4 of six models.

Test points	π1	π2	π3	π4
1	704.04	1.05	1.9	62.3
2	704.04	1.05	1.9	89.4
3	704.04	1.05	1.9	55168.4
4	704.04	1.05	1.9	83581.6
5	704.04	1.05	1.9	159777.3
6	704.04	1.05	1.9	118928.6

Procedure for experimentation

The main objective of the proper procedure of experimentation is to mitigate the error which aggrandizes the desired results.

To generate the vibrations in the bearing cap a load torque has to be applied on shaft S2. Hence, a varying load condition can be obtained by applying different dead weights at load drum. However, to see

the effect of different misalignment conditions on the vibration spectrum the following procedure is adopted.

1. At the genesis of the experimentation, the vibration spectrums have been gathered from two bearings B1 and B2 without taking any misalignment and loading condition on 1100 rpm.
2. Next to this, the load of 1 kg is applied on the load drum for applying load torque and again the vibrations spectrums from two bearings are gathered on 1100 rpm.
3. Now the speed has changed to 1440 rpm and the vibration spectrums are obtained from bearings B1 and B2.
4. The load of one kg is applied on the load drum and on the same speed of 1440 rpm vibration spectrums have been gathered.
5. The steps 1, 2, 3, and 4 enlisted above are repeated by giving 1 mm misalignment laterally to bearing B1. Thus vibration spectrums for each step for two bearings are gathered.
6. The steps 1, 2, 3, and 4 enlisted above are again repeated by giving 2 mm misalignment laterally to bearing B1. Thus vibration spectrums for each step for two bearings are gathered.

Therefore, there are twelve vibration spectrums for each bearing have been gathered.

3.3.4. Data generation

It was decided to take vibration readings in lateral and radial direction of the bearings by FFT analyzer and accelerometer [57]. The speed of shaft is also measured.

Table 5. Values of amplitudes at different coupling frequencies at horizontal position for Bearing B1 (Velocity mode)

V (mm/sec)	1X (one times rpm of shaft)	2X (two times rpm of shaft)	3X (three times rpm of shaft)
1.	0.9	0.2	0.8
2.	1.55	0.3	1.2
3.	6	1	1.5
4.	1.1	0.2	1
5.	1.25	0.5	1
6.	1.1	0.1	1.9
7.	5	0.8	2
8.	1.4	0.5	2
9.	1.2	1	1.2
10.	0.15	0.2	0.19
11.	0.8	1	0.9
12.	1.2	0.25	1.2

In addition, time taken for vibration spectrum for each bearing is also noted down. For different coupling frequencies twelve sets of vibration amplitudes are noted down for each bearing. The relevant spectrums are given in Appendix A. The values of amplitudes are given in Table 10 and Table 11.

Table 6. Values of amplitudes at different coupling frequencies at a vertical position for Bearing B1 (Velocity mode)

V(mm/sec)	X1	X2	X3
1.	0.2	0.33	0.65
2.	0.1	0.3	0.8
3.	0.5	2.3	0.6
4.	0.3	0.4	0.48
5.	0.2	0.3	0.68
6.	0.8	0.28	1.1
7.	0.8	1.4	0.7
8.	0.2	0.4	1
9.	0.1	0.6	1.1
10.	0.24	0.18	0.24
11.	0.3	0.8	0.5
12.	0.2	0.3	1.2

3.3.5. Model formulation by identifying the constant and various indices of pi terms

Let the prototype designed of the following form

$$(\pi)=K\left((\pi_1)^a(\pi_2)^b(\pi_3)^c(\pi_4)^d\right) \quad (9)$$

The regression equations become as bellow:

$$\sum Y=nK1+a\sum A+b\sum B+c\sum C+d\sum D \quad (10)$$

$$\sum YA=K1\sum A+a\sum A^2+b\sum AB+c\sum AC+d\sum AD \quad (11)$$

$$\sum YB=K1\sum B+a\sum AB+b\sum B^2+c\sum BC+d\sum BD \quad (12)$$

$$\sum YC=K1\sum C+a\sum AC+b\sum BC+c\sum C^2+d\sum CD \quad (13)$$

$$\sum YD=K1\sum D+a\sum AD+b\sum BD+c\sum CD+d\sum D^2 \quad (14)$$

In the former equivalences n is the number of sets of readings, A, B, C, D represents the impartial pi terms log π1, log π2, log π3, and log π4 whilst Y represents log (π).

The following matrix represents the equations, which is used for programming.

$$[Y]=[X]\ x[a] \quad (15)$$

The equations for the corresponding models are formed as under:

$1X_h$ model

$$Y=1(\pi 1)^{-.949}(\pi 2)^{-2.025}(\pi 3)^{1.08}(\pi 4)^{-.0879} \quad (16)$$

$2X_h$ model

$$Y=1\ (\pi 1)^{-1.23}X\ (\pi 2)^{0.7174}X\ (\pi 3)^{.3359}X\pi\ (4)^{.0124} \quad (17)$$

$3X_h$ model

$$Y=1 * (\pi 1)^{-.894} * (\pi 2)^{-1.15} * (\pi 3)^{-.198} * (\pi 4)^{-.0272} \quad (18)$$

$1X_v$ model

$$Y=1 * (\pi 1)^{-1.507} * (\pi 2)^{-4.379} * (\pi 3)^{2.65} * (\pi 4)^{.0768} \quad (19)$$

$2X_v$ model

$$Y=1 * (\pi 1)^{-1.12} * (\pi 2)^{-0.7749} * (\pi 3)^{.1279} * (\pi 4)^{-.0235} \quad (20)$$

$3X_v$ model

$$Y=1 * (\pi 1)^{-1.266} * (\pi 2)^{-3.93} * (\pi 3)^{2.526} * (\pi 4)^{.0244} \quad (21)$$

4. ANALYSIS OF THE MATHEMATICAL MODEL

This section emphasizes on the discussions about qualitative and quantitative analysis of the mathematical models [58]-[59].

4.1. Quantitative analysis of model

The mathematical models constructed in the preceding section are provided here for clarification.

$$Y=1 * (\pi 1)^{-.949} * (\pi 2)^{-2.025} * (\pi 3)^{1.08} * (\pi 4)^{-.0879} \quad (22)$$

$$Y=1 * (\pi 1)^{-1.23} * (\pi 2)^{0.7174} * (\pi 3)^{.3359} * (\pi 4)^{.0124} \quad (23)$$

$$Y=1 * (\pi 1)^{-.894} * (\pi 2)^{-1.15} * (\pi 3)^{-.198} * (\pi 4)^{-.0272} \quad (24)$$

$$Y=1 * (\pi 1)^{-1.507} * (\pi 2)^{-4.379} * (\pi 3)^{2.65} * (\pi 4)^{.0768} \quad (25)$$

$$Y=1 * (\pi 1)^{-1.12} * (\pi 2)^{-0.7749} * (\pi 3)^{.1279} * (\pi 4)^{-.0235} \quad (26)$$

$$Y=1 * (\pi 1)^{-1.266} * (\pi 2)^{-3.93} * (\pi 3)^{2.526} * (\pi 4)^{.0244} \quad (27)$$

The interpretation of the aforementioned models is given in terms of multiple elements, including
(1) the order of effect of inputs upon outputs
(2) Explanation of the fitting curve constant K.

Equation (22) indicates that π_2 term, which relates to elasticity characteristics of experimental set-up, has highest influence as -2.025 whilst, the least influence is seen for π4 as -0.0879, which relates to dynamic characteristics of experimental set-up.

The π1, π3 relates to mass moment of inertia and equivalent length has moderate influence as -0.949 and 1.08 respectively.

Similarly, interpretation for other models is provided in appendix. The values of curve fitting constant in these models are 1. This indicates the aggregate influence of all extraneous factors. Furthermore, because it is positive, it implies that there are a large number of reasons that have an impact on the rising effect.

4.2. Qualitative analysis of model

The quantitative analysis consists of three parts: (1) sensitivity analysis, (2) model optimization, and (3) model reliability.

4.2.1. Sensitivity analysis for model 1Xh

The sensitivity for model $1X_h$ is evaluated and discussed below. However, sensitivity for other models is given in Appendix B.

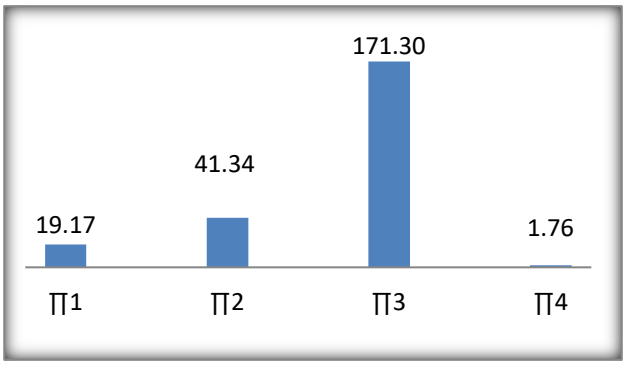

Figure 7. Sensitivity Graph of independent pi terms for model 1Xh

When a total of 20% change is given in the independent term 3, the value of the dependent pi term (Y) (estimated from model) changes by 171.30%, according to the model (Equation 16). However, the lowest variation of the dependent pi term (Y) is observed, which is 1.7 percent. This variation is related to the pi term 4. Similarly, a change of about 19.7 percent and 41.34 percent is seen due to changes in the values of π1 and π2, respectively as shown in Figure 7.

If one closely observes the rate of change in the dependent pi term with the influence of Independent Pi terms, it is noted that the independent term π3 causes the greatest change in the dependent pi term. Whereas pi term 4 is accountable for the lowest number of variation in the dependent pi term. As a result, π3 is the most sensitive pi word, whereas π4 is the least sensitive pi term. In descending order of sensitivity, the sequence of the different pi terms is π3, π2, π1, π4.

4.2.2. Optimization of model

The present work is focused on obtaining not merely to formulate a mathematical prototype but to come up with best set of impartial variables.

This in turn will facilitate us to satisfy quantitative function i.e minimization of the vibration amplitude.

For optimization of model the presented nonlinear mathematical paradigm of reliant Pi term needs to be transformed to linear form.

It can be converted by taking log on both the sides of the mathematical equivalence of the prototype.

For the dependent π term, we have

$$(\pi) = K * [(\pi 1)^a \ (\pi 2)^b \ (\pi 3)^c \ (\pi 4)^d \ ] \quad (28)$$

Taking Log on both the side of this equation,

$$\text{Log } (Y) = \text{Log } K + a \text{ Log } (\pi 1) + b \text{ Log } (\pi 2) + c \text{ Log } (\pi 3) + d \text{ Log}(*(\pi 4) \quad (29)$$

Let, Log (Y)=Z; Log K=K; Log(π1)=X1; Log (π2)=X2 ; Log (π3)=X3, Log(*(π4)=X4;

The linear model in the form of a polynomial of the first degree may therefore be expressed as,

$$Z = k + a * X1 + b * X2 + c * X3 + d * X4 \quad (30)$$

Now equation 30 is processed further with the objective being minimization of quantitative function i.e. vibration amplitude.

The constraints for the variables can be chosen from the set of reading formed for autonomous pi terms as minimum and maximum values.

Thus, log(π1 min) and log(π1 max), are the minimum and maximum value of individual pi term which represents first two constraints for the challenge. Let C1= Log π1 max, and C2= Log π1 min.

As a result, the constraint equation becomes.

$$1*X1 + 0*X2 + 0*X3 + 0*X4 \leq C1 \quad (31)$$

$$1*X1 + 0*X2 + 0*X3 + 0*X4 \geq C2 \quad (32)$$

The other constraints are discovered to be as well.

$$0*X1 + 1*X2 + 0*X3 + 0*X4 \leq C3 \quad (33)$$

$$0*X1 + 1*X2 + 0*X3 + 0*X4 \geq C4 \quad (34)$$

$$0*X1 + 0*X2 + 1*X3 + 0*X4 \leq C5 \quad (35)$$

$$0*X1 + 0*X2 + 1*X3 + 0*X4 \geq C6 \quad (36)$$

$$0*X1 + 0*X2 + 0*X3 + 1*X4 \leq C7 \quad (37)$$

$$0*X1 + 0*X2 + 0*X3 + 1*X4 \geq C8 \quad (38)$$

Now for the present linear software design problem MS solver is used. Furthermore, the values of the dependant and independent pi terms may be obtained by calculating the antilog of Z, X1, X2, X3, and X4.

For model $X1_h$

Z=-2.603361348;
X1=2.847597334;
X2=0.021189299;
X3=0.278753601;
X4=1.794138357;

Hence, Z_{min}= $(Y)_{min}$ = antilog (-2.603361348) =.0025and corresponding values of independent pi terms are obtained by taking the antilog of X1, X2, X3 and X4. These values are 703.88, 1.049, 1.899, and 62.24.

For model $X2_h$

Z=-2.603361348;
X1=2.847597334;
X2=0.021189299;
X3=0.278753601;
X4=1.794138357;

Hence, Z_{min}= $(Y)_{min}$ =antilog (-2.60336)=.00254. Taking the antilog of X1, X2, X3, and X4 yields the equivalent values of independent pi terms. These values are 703.07, 1.049, 1.89, and 62.24.

For model $X3_h$

Z=-2.603361348;
X1=2.847597334;
X2=0.021189299;
X3=0.278753601;
X4=1.794138357;

Hence, Z_{min} = $(Y)_{min}$ = antilog (-2.603361348) =.0025. Taking the antilog of X1, X2, X3, and X4 yields the equivalent values of independent pi terms. These values are 703.88, 1.049, 1.899, and 62.24.

For model $X1_v$

Z=-2.603361348;
X1=2.847597334;
X2=0.021189299;
X3=0.278753601;
X4=1.794138357;

Hence, Z_{min} = $(Y)_{min}$ =antilog (-2.603361348) =.0025. Taking the antilog of X1, X2, X3, and X4 yields the equivalent values of independent pi terms. These values are 703.88, 1.049, 1.899, and 62.24

For model $X2_v$

Z=-2.603361348;
X1=2.847597334;
X2=0.021189299;
X3=0.278753601;
X4=1.794138357;

Hence, $Z_{min} = (Y)_{min}$ =antilog (-2.603361348) =.0025. Taking the antilog of X1, X2, X3, and X4 yields the equivalent values of independent pi terms. These values are 703.88, 1.049, 1.899, and 62.23.

For model $X3_v$

Z=-2.603361348;
X1=2.847597334;
X2=0.021189299;
X3=0.278753601;
X4=1.794138357;

Hence, $Z_{min} = (Y)_{min}$ = antilog (-2.603361348) =.0025. Taking the antilog of X1, X2, X3, and X4 yields the equivalent values of independent pi terms. These values are 703.88, 1.049, 1.899, and 62.23.

4.2.3 Reliability of model

The reliability term is pertaining to the chance of failure. Indeed, consistency indicates performance of model.

The mean error can be used to determine reliability [60]. This may be accomplished by employing the following formula,

$$\text{Reliability}=1-\text{Mean error} \quad (39)$$

Where,

- Mean error= ΣXIFI/ ΣFI
- ΣFI=The frequency of error incidence is totaled and
- ΣXIFI= Product summation for frequency of error occurrence and percentage of error.

Hence reliabilities obtained for six models in percentage are 99.372945, 99.978246, 99.877723, 99.964791, 99.989411, and 99.923031.

5. RESULT AND DISCUSSION

Elastomeric or flexible element is placed between the hubs to cope with misalignment in the system.

The flexible elements is being operated under different loads i.e driving torque from motor and load due to misalignment which results into low vibration and protects other machine components from failures.

$1X_h$ model indicates that π_2 term, which relates to elasticity characteristics of experimental set-up, has highest influence as -2.025 whilst, the least influence is seen for π4 as -0.0879, which relates to dynamic characteristics of experimental set-up.

The π1, π3 relates to mass moment of inertia and equivalent length has moderate influence as -0.949 and 1.08 respectively. Similarly, interpretation for other models is provided in appendix.

6. CONCLUSIONS:

Through the present work, an attempt has been made to understand the relationship between the amount of misalignment and the growth of amplitude.

From the rigorous study, it has been revealed that it falls under the non-linear domain. Therefore, further attempts are needed to be executed as a future adjent proposal.

This paper tries to understand the behavior of coupling vibrations b formulating predictive mathematical models.

The proportionality constant for each mathematical model is one. Therefore, one can say that all possible extraneous variables have been accounted for well.

The influence of all indices over dependent variables revealed that the π3 term is more influential as the location of inertias plays an important role in inducing the bearing reaction, which culminates into non-linear vibrations.

The corroboration with the qualitative analysis discussed in former statements is executed through sensitivity analysis, which shows that the π3 term is more sensitive for the present research.

The optimization analysis is executed to ascertain the minimum vibration level for the present case, and the values are obtained below the alarming level.

The quality model is proven as the models predicted the vibrations at the tune of 99 % reliability.

ACKNOWLEDGMENTS

This study received no particular financing from funding agencies in the public, commercial, or non-profit sectors.

REFERENCE:

[1] J.K. Sinha, Health Monitoring Techniques for Rotating Machinery, Ph.D. Thesis, University of Wales Swansea, Swansea, 2002.

[2] Minda, A., Gillich, G., Budai, A. And Vasile, O. 2019. The Study of Vibration Transmission Using Virtual Instruments. *Romanian Journal of Acoustics and Vibration*. 15, 2 (Jan. 2019), 143-148.

[3] Upmanyu, A., Dhiman, M., Gupta, D., Kakkar, M., Singh, K. And Singh, D. 2020. Frequency Dependence Studies of Acoustical and Thermo-Dynamical Parameters of The Binary Mixtures of Isopropyl Sulphide And Acetic Acid. *Romanian*

Journal of Acoustics and Vibration. 17, 2 (Dec. 2020), 128-134.

[4] Kumar S., Mitra A., Roy H., Geometrically nonlinear free vibration analysis of axially functionally graded taper beams, Engineering Science and Technology, an International Journal, Vol. 18, 2015, pp. 579-593.

[5] Mehta, G., Deogirkar, S., Borkar, P., Shelare, S., And Sontakke, S. 2019. Estimation of Vibration Response of a Bridge Column. *SSRN Electronic Journal*., 1283-1290. doi:10.2139/ssrn.3356326

[6] Vlase, S., Itu, C., Vasile, O., Năstac, C., Stanciu, M. And Scutaru, M. 2018. Vibration Analysis of a Mechanical System Composed of Two Identical Parts. *Romanian Journal of Acoustics and Vibration*. 15, 1 (Aug. 2018), 58-63.

[7] Dewell DL and Mitchell L D (1984) Detection of a misaligned disk coupling using spectrum analysis. *ASME Trans. Journal Vibration, Acoustics, Stress and Reliability Design* 106 : 9-16.

[8] Antoni, J., 2007. "Fast computation of the kurtogram for the detection of transient faults". *Mechanical Systems and Signal Processing*, 21, pp. 108 – 124.

[9] Imran, M., Khan, R. and Badshah, S. 2018. Vibration Analysis of Cracked Composite Laminated Plate and Beam Structures. *Romanian Journal of Acoustics and Vibration*. 15, 1 (Aug. 2018), 3-13.

[10] Jackson C (1973) Cold and Hot Alignment Techniques of Turbo machinery. Proceeding 2nd Turbo machinery Symposium, Turbo machinery Laboratory, Texas A and M University Texas.

[11] Shchelkunov, E. B., Shchelkunova, M. E., Ryabov, S. A., & Glinka, A. S. (2021). Parallel Mechanisms with Flexible Couplings. Russian Engineering Research, 41(7), 593–597. doi:10.3103/s1068798x21070236

[12] Khatkhate, A., Gupta, S., Ray, A., & Patankar, R. (2008). Anomaly detection in flexible mechanical couplings via symbolic time series analysis. Journal of Sound and Vibration, 311(3-5), 608–622. doi:10.1016/j.jsv.2007.09.046

[13] Alfouneh, M., & Tong, L. (2018). Damping Design of Flexible Structures With Graded Materials Under Harmonic Loading. Journal of Vibration and Acoustics, 140(5). doi:10.1115/1.4039571.

[14] Stanica, C., Predoi, M. and Stroe, I. 2020. Study of Rotating Machineries in A Non-Inertial Reference Frame Subjected to Rotations. *Romanian Journal of Acoustics and Vibration*. 16, 2 (Apr. 2020), 125-136.

[15] Itu C, Bratu P, Borza Pn, Vlase S, Lixandroiu D. 2020. Design and Analysis of Inertial Platform Insulation of the ELI-NP Project of Laser and Gamma Beam Systems. *Symmetry*. 12(12), 1-22. https://doi.org/10.3390/sym12121972.

[16] Hashemi Kachapi, S.H. 2020. Vibration and Stability Analysis of Multi Walled Piezoelectric Nanoresonator. *Romanian Journal of Acoustics and Vibration*. 17, 2 (Dec. 2020), 135-148.

[17] Randall, R., and Sawalhi, N., 2011. "Use of the cepstrum to remove selected discrete frequency components from a time signal". *Rotating Machinery, Structural Health Monitoring, Shock and Vibration*, Volume 5: Proceedings of the 29th IMAC, A Conference on Structural Dynamics, 2011, 5, pp. 451 – 461.

[18] S. Edwards, A.W. Lees, M.I. Friswell, Fault diagnosis of rotating machinery, *Shock and Vibration Digest* 30 (1998) 4–13.

[19] [19] A. Muszynska, Rotor to stationary element rub-related vibration phenomena in rotating machinery—literature survey, *Shock and Vibration Digest* 21 (1989) 3–11.

[20] W.C. Foiles, P.E. Allaire, E.J. Gunter, Review: rotor balancing, *Shock and Vibration* 5 (1998) 325–336.

[21] A.G. Parkinson, Balancing of rotating machinery, *IMechE Proceedings C—Journal of Mechanical Engineering Science* 205 (1991) 53–66.

[22] Schweitzer G and Maslen E H 2009 Magnetic bearings: theory, design, and application to rotating machinery. *Berlin: Springer*

[23] A.W. Lees, Misalignment in rigidly coupled rotors, *J. Sound Vib.* 305 (1) (2007) 261–271.

[24] Zhao, X. 2020. Exact Vibration Analysis of Beams with Arbitrary Intermediate Elastic Supports, Concentrated Masses and Non-Classical Boundary Conditions Under an Axial Force Using Shape Function Method. *Romanian Journal of Acoustics and Vibration.* 17, 1 (Nov. 2020), 57-76.

[25] G. Simon, Prediction of vibration behaviour of large turbo-machinery on elastic foundations due to unbalance and coupling misalignment, *Proceedings of the Institution of Mechanical Engineers, Part C—Journal of Mechanical Engineering Science* 206 (1992) 29–39.

[26] Eaga, A., Bhosale, S. and Mali, K. 2020. Formulation of Statistical Model to Determine Natural Frequencies of the Cantilever Beam for Linear Variation of Circular Perforation Along the Length. *Romanian Journal of Acoustics and Vibration.* 16, 2 (Apr. 2020), 106-112

[27] S.K. Kuppa, M. Lal, Characteristic parameters estimation of active magnetic bearings in a coupled rotor system, *ASME J. Verification Validation Uncertainty Quantification* 4 (3) (2019) 1–11.

[28] S.K. Kuppa, M. Lal, Dual flexible rotor system with active magnetic bearings for unbalance and coupling misalignment faults analysis, *Sadhana, Indian Acad. Sci.* 44 (188) (2019) 1–16.

[29] M. Lal, R. Tiwari, Multi-fault identification in simple rotor-bearing-coupling systems based on forced response measurements, *Mech. Mach. Theory* 51 (2012) 87–109.

[30] M. Lal, R. Tiwari, Quantification of multiple fault parameters in flexible turbo-generator systems with incomplete rundown vibration data, *Mech. Syst. Sig. Process*. 41 (1–2) (2013) 546–563.

[31] M. Vishwakarma, R. Purohit, V. Harshlata, P. Rajput, Vibration analysis & condition monitoring for rotating machines: a review, *Mater. Today:. Proc*. 4 (2) (2017) 2659–2664.

[32] N. Sawalhi, S. Ganeriwala, M. Toth, Parallel misalignment modeling and coupling bending stiffness measurement of a rotor-bearing system, *Appl. Acoust*. 144 (2019) 124–141.

[33] S.K. Kuppa, M. Lal, December. Characteristic parameter estimation of AMB supported coupled rotor system. *In ASME 2017 Gas Turbine India Conference, American Society of Mechanical Engineers* (2017).

[34] S.K. Kuppa, M. Lal, September. Characteristic Parameters Estimation of Uncertainties Present in an Active Magnetic Bearing Integrated Flexible Rotor System Using Dynamic Reduction Technique, In *International Conference on Rotor Dynamics,* Springer, Cham (2018) 234-248.

[35] M. Lal, M. Satapathy, Estimation of speed dependent fault parameters in a coupled rotor-bearing system, *Archiv. Mech. Eng*. 65 (3) (2018) 327–347.

[36] I. Chatzisavvas, F. Dohnal, Unbalance identification using the least angle regression technique, *Mech. Syst. Sig. Process*. 50 (2015) 706–717.

[37] J.J. Carbajal-Hernández, L.P. Sánchez-Fernández, I. Hernández-Bautista, J.D.J. Medel-Juárez, L.A. Sanchez-Perez, Classification of unbalance and misalignment in induction motors using orbital analysis and associative memories, *Neurocomputing* 175 (2016) 838–850.

[38] X.Q. Fu, W.T. Jia, H. Xu, S.L. Song, Imbalance–misalignment–rubbing coupling faults in hydraulic turbine

vibration, *Optik-Int. J. Light Electron Optics* 127 (8) (2016) 3708–3712.
[39] M. Lal, Multiple fault parameter estimation of a fully assembled turbo generator system, *Archiv. Mech. Eng.* 65 (2) (2018) 223–252.
[40] Sabir, Y., Brahmi, A. and Gauthier, C. 2021. A Mathematical Method for Harmonizing the Vibrations of Compound Cymbals. *Romanian Journal of Acoustics and Vibration.* 18, 1 (Jul. 2021), 18-25
[41] Gibbons C (1976) Coupling Misalignment Forces. *Proceeding 5th Turbo machinery Symposium, Turbo machinery Laboratory*, Texas A and M University Texas.
[42] Minda, A., Barbinita, C.-I. and Gillich, G. 2020. A Review of Interpolation Methods Used for Frequency Estimation. *Romanian Journal of Acoustics and Vibration*. 17, 1 (Nov. 2020), 21-26.
[43] Piotrowski, J (1995) Shaft Alignment Hand-book : Marcel *Dekker Book Publishers*.
[44] Hariharan V and Srinivasan PS (2010) Vibrational Analysis of Flexible Coupling by Considering Unbalance. *World Applied Sciences Journal* 8 (8) : 1022-1031.
[45] Koohestani, S. 2018. Investigation of the Effect of an Inconsistent Blade on Natural Frequencies of a Rotating Multi Blade System. *Romanian Journal of Acoustics and Vibration*. 15, 1 (Aug. 2018), 33-40.
[46] Sinhaa. JK, Leesb AW and Friswellc MI (2004) Estimating unbalance and misalignment of a flexible rotating machine from a single run-down. *Journal of Sound and Vibration* 272 : 967–989.
[47] Xu M and Marangoni RD (1994) Vibration analysis of a motor flexible coupling rotor system subject to misalignment and unbalance. Journal of Sound Vibration 176(5) : 663-679.
[48] Shiwalkar B D (2010) Design for Machine Elements : *Denett and Company Publishers*.
[49] Wowk Victor (1991) Machinery Vibration (Measurement and Analysis) : *Mcgraw Hill Publishers*.
[50] Shelare, S. D., Kumar, R., & Khope, P. B. (2020). Formulation of a Mathematical Model for Quantity of Deshelled Nut in Charoli Nut Deshelling Machine. *Advances in Metrology and Measurement of Engineering Surfaces*, 89–97. doi:10.1007/978-981-15-5151-2_9
[51] Sekhar AS and Prabhu BS (1995) Effect of Coupling Misalignment on Vibrations of Rotating Machinery. *Journal of Sound and Vibration* 185(4) : 655-671.
[52] Schenck H (1967) Theories of Engineering Experimentation : *McgrawHill Publishers*.
[53] Belkhode, P. N. (2017). Mathematical Modelling of Liner Piston Maintenance Activity using Field Data to Minimize Overhauling Time and Human Energy Consumption. *Journal of The Institution of Engineers (India): Series C*, 99(6), 701–709. doi:10.1007/s40032-017-0377-7
[54] Waghmare, S. N., Shelare, S. D., Tembhurkar, C. K., & Jawalekar, S. B. (2020). Development of a Model for the Number of Bends During Stirrup Making Process. *Advances in Metrology and Measurement of Engineering Surfaces*, 69–78. doi:10.1007/978-981-15-5151-2_7
[55] Dhutekar, P., Mehta, G., Modak, J., Shelare, S., & Belkhode, P. (2021). Establishment of mathematical model for minimization of human energy in a plastic moulding operation. Materials Today: Proceedings. doi:10.1016/j.matpr.2021.05.330
[56] P.B. Khope, S.D. Shelare, Prediction of torque and cutting speed of pedal operated chopper for silage making, *Adv. Industr. Mach. Mech.* 89–97 (2021), https://doi.org/10.1007/978-981-16-1769-0_22.
[57] Jain, V. K. (2018). Interpolated FFT Harmonic Analyzer for Power Systems, and System on a Chip (SOC) for It. *SoutheastCon 2018*. doi:10.1109/secon.2018.8479077
[58] Belkhode, P. N. (2019). Development of mathematical model and artificial neural network simulation to predict the performance of manual loading operation of underground mines. *Journal of Materials Research and Technology*, 8(2), 2309–2315. doi:10.1016/j.jmrt.2019.04.015
[59] Mowade, S., Waghmare, S., Shelare, S., & Tembhurkar, C. (2019). Mathematical Model for Convective Heat Transfer Coefficient During Solar Drying Process of Green Herbs. *Computing in Engineering and Technology*, 867–877. doi:10.1007/978-981-32-9515-5_81
[60] Waghmare, S. N., Sakhale, C. N., Tembhurkar, C. K., & Shelare, S. D. (2019). Assessment of Average Resistive Torque for Human-Powered Stirrup Making Process. *Computing in Engineering and Technology*, 845–853. doi:10.1007/978-981-32-9515-5_79